References

CRUICKSHANK, D. W. J. (1949). *Acta Cryst.* **2**, 65.
EHRLICH, P. (1949). *Z. anorg. Chem.* **260**, 1.
GRØNVOLD, F. (1955). *Tidskr. Kjemi, Bergvesen, Met.* **15**, 49.
GRØNVOLD, F., HAGBERG, O. & HARALDSEN, H. (1958). *Acta Chem. Scand.* **12**, 971.
HAHN, H. & NESS, P. (1957). *Naturwiss.* **44**, 581.
HAHN, H. & NESS, P. (1959). *Z. anorg. Chem.* **302**, 17.
Internationale Tabellen zur Bestimmung von Kristallstrukturen (1935). Berlin: Borntraeger.
JELLINEK, F. (1957). *Acta Cryst.* **10**, 620.
LEVINGER, B. V. (1953). *Trans. Amer. Soc. Metals*, **197**, 195.
OKAZAKI, A. & HIRAKAWA, K. (1956). *J. Phys. Soc., Japan*, **11**, 930.
PAULING, L. (1947). *J. Amer. Chem. Soc.* **69**, 542.
PEDERSEN, B. (1958). Thesis, University of Oslo.
RAAUM, F. (1959). Thesis, University of Oslo.

Acta Cryst. (1961). **14**, 934

Experimental Atomic Scattering Factors and Anomalous Dispersion Corrections for Th, U, and Pu*†

BY R. B. ROOF, JR.

Los Alamos Scientific Laboratory, University of California, Los Alamos, New Mexico, U.S.A.

(*Received* 20 *September* 1960)

Experimental atomic scattering factors have been determined for Th, U, and Pu with Mo $K\alpha$, Cu $K\alpha$, Fe $K\alpha$, and Cr $K\alpha$ X-radiations. The Thomas–Fermi-Dirac scattering curves were used as a theoretical basis, and the difference between the experimental and TFD curves was taken as a measure of the anomalous dispersion correction.

As a result of determining the scattering factors for Th, U, and Pu from experimental samples of ThO_2, UO_2, and PuO_2, the scattering factor for oxygen was also determined. The experimentally derived scattering curve for oxygen is in good agreement with the theoretical scattering curve for oxygen according to McWeeney.

Calculated values for $\Delta f'$ and $\Delta f''$, the real and imaginary portions of the anomalous dispersion correction are compared with experimental values for these quantities. Agreement can be described as semi-quantitative since the experimental terms are of the same order of magnitude and have the same signs as those indicated by theory.

Introduction

Accurate atomic scattering factors are essential for any careful study of interatomic distances and thermal vibration parameters by diffraction methods. Because of the interest in this laboratory in precise studies of the structures of intermetallic and other compounds of various heavy metals, the atomic scattering factors of Th, U, and Pu have been determined experimentally for Mo, Cu, Fe, and Cr $K\alpha$ X-radiations.

The Thomas–Fermi–Dirac scattering curves are used as a theoretical basis, and the difference between the experimental curves and the TFD curves is taken as a measure of the anomalous dispersion correction. The L_{III} absorption edges of Th, U, and Pu lie very close to Mo $K\alpha$ radiation, and the M_I, M_{II} absorption edges of these elements are close to Fe $K\alpha$ and Cr $K\alpha$ radiation respectively. Since no really sound theoretical treatment of anomalous dispersion for the L and M electrons has been developed, the agreement between the experimental and calculated values for anomalous dispersion in this region must be described as qualitative or at best semi-quantitative. Furthermore, any theoretical treatment is complicated because the L and M absorption edges themselves are quite complex.

Experimental theory

The atomic scattering factors of Th, U, and Pu were experimentally determined by utilizing techniques first proposed by the author (Roof, 1959*a*), corrected by Chipman and Paskin (1960), and subsequently revised by the author (Roof, 1960*a*). A brief description of these experimental techniques is given in the following paragraphs.

The experimental samples consisted of a powdered material having the geometrical shape of a slab. The equation relating the atomic scattering factor of a material having the shape of a slab to experimental

* Work done under the auspices of the United States Atomic Energy Commission.

† A brief summary of this paper was presented at the Fifth Congress of the International Union of Crystallography at Cambridge, England, August, 1960.

measurements of reflected X-ray intensities has the following form:

$$\frac{\Sigma\omega}{I_0} = |F_0|^2\left(\frac{e^2}{mc^2}\right)^2\left(\frac{\lambda^3}{64\pi}\right)\left(\frac{\varrho}{\mu}\right)\left(\frac{1+\cos^2 2\theta}{\sin^2\theta\cos\theta}\right)\left(N^2\right)\left(\frac{l}{r}\right) \quad (1)$$

where

Σ = integrated intensity of a reflection, counts,
ω = angular velocity of the detector, sec.$^{-1}$,
I_0 = intensity of the incident beam, c.p.s,
$|F_0|$ = the structure factor per unit cell,
l = height of detector slit, cm.,
r = distance from specimen to detector, cm.,
$(e^2/mc^2)^2$ = $7{\cdot}9402 \pm 0{\cdot}0005 \times 10^{-26}$ cm.^{2},
λ = wavelength of incident radiation in cm.,
ϱ = multiplicity factor,
μ = theoretical linear absorption coefficient, cm.$^{-1}$,
$(1+\cos^2 2\theta/\sin^2\theta\cos\theta)$ = combined Lorentz-polarization factor,
N = number of unit cells per unit volume.

In order to determine $|F_0|$, and hence obtain an observed scattering factor from equation (1), a monochromatic wavelength is required, as is data concerning μ, Σ, I_0, and the constants.

A monochromatic wavelength is obtained by operating the X-ray tube at a voltage sufficiently high to generate the characteristic $K\alpha$ and $K\beta$ radiation but low enough so that $\lambda \leqq K\alpha/2$ is not generated; then the $K\beta$ radiation is filtered from the X-ray beam leaving only the characteristic $K\alpha$ radiation.

The theoretical linear absorption coefficient, μ, is obtained by multiplying the mass absorption coefficient by the theoretical density.

The integrated intensity, Σ, of a reflection is obtained by determining the total number of counts in traversing from one side of a reflection to the other and then subtracting the number of background counts.

The intensity of the incident beam, I_0, is determined by the multiple foil, linear absorber technique. For low values of n (the number of foils) coincidence losses cause I (the measured intensity) to deviate from a straight line, and, therefore, the measured I for $n=0$ does not accurately represent I_0. I_0 is found by extrapolating the linear portion of a plot of log I *vs.* n to $n=0$.

In order to reduce to a negligible value the random variations in day to day operation of an X-ray unit, a separate value of I_0 was computed for each integrated intensity, Σ, measured for any reflection.

The observed structure factor squared, $|F_0|^2$, obtained from equation (1), is corrected for the effect of temperature by multiplying by $(\exp 2B\sin^2\theta/\lambda^2)$ where $2B$ is determined from the Debye characteristic temperature according to:

$$2B = 12h^2T(\Phi x + \tfrac{1}{4}x)/mk\Theta^2 \quad (2)$$

where

h = Planck's constant, $6{\cdot}6252 \pm 0{\cdot}0005 \times 10^{-27}$ erg.-sec.,
m = average mass of a lattice point, g,
T = temperature, °K.,
Θ = characteristic temperature, °K.,
k = Boltzmann's constant, $1{\cdot}38042 \pm 0{\cdot}00010 \times 10^{-16}$ erg.-deg.$^{-1}$,
$x = \Theta/T$, and
Φx = Debye function.

The observed structure factor squared and corrected for temperature, $|F_T|^2$, should now be corrected for the effects of surface roughness, and for primary and secondary extinction. Since the present experimental samples consisted of small, nearly equidimensional particles and were formed in the shape of slabs the surfaces of which were metallographically polished, the effects of surface roughness, and primary and secondary extinction were assumed to be negligible.

The structure factor squared, corrected for temperature, $|F_T|^2$, is related to the atomic scattering factor, f_j, by

$$|F_T|^2 = \{\sum_j |f_j| G_j\}^2 \quad (3)$$

where G_j is the geometrical portion of the structure factor equation and in general is equal to

$$(\exp -2\pi i(hx_j + ky_j + lz_j)) .$$

The atomic scattering factor derived from the above expression must be modified by using the anomalous dispersion correction in order to obtain a true atomic scattering factor. The relationship between the true atomic scattering factor and the anomalous dispersion correction is given by the complex quantity

$$f = f_0 + \Delta f' + i\Delta f'' \quad (4)$$

where f = atomic scattering factor corrected for dispersion, f_0 = true atomic scattering factor, $\Delta f'$ = real part of dispersion correction, and $\Delta f''$ = imaginary part of dispersion correction.

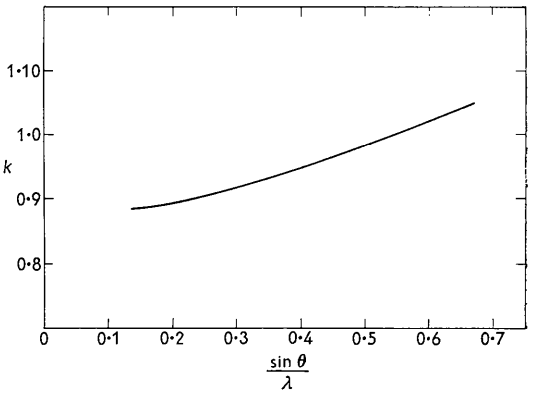

Fig. 1. Variation of an instrument calibration constant, k, as a function of $\sin\theta/\lambda$. The quantity k is derived from a comparison of an observed scattering factor for aluminum with the theoretical scattering factor (Parry, 1955) for aluminum.

Application of the techniques described above to a slab of powdered aluminum (Roof, 1959*a*) resulted in an observed value of the atomic scattering factor, f(obs.), which may be compared (Roof, 1960*a*) with a theoretical value of the atomic scattering factor, f(theo.), according to

$$f(\text{theo.}) = kf(\text{obs.}) \tag{5}$$

where k is defined as an instrument calibration constant. The variation of k as a function of $\sin\theta/\lambda$ is shown in Fig. 1 and was derived from a comparison of the observed scattering factor of aluminum with the theoretical scattering factor for aluminum according to Parry (1955).

Experimental method

Intensity measurements were made at room temperature with a General Electric XRD-5 diffraction unit equipped with a 1° incident beam slit, a 0·2° detector slit, and medium resolution Soller slits. Four wave lengths were employed, Mo $K\alpha$, Cu $K\alpha$, Fe $K\alpha$, and Cr $K\alpha$. Proportional counter tubes were used to detect the X-radiation. A krypton-filled proportional tube was used for Mo, and an argon-filled proportional tube was used for Cu, Fe, and Cr. Pulse height analysis was used to discriminate against unwanted radiation.

The samples consisted of pressed and sintered slabs of powdered ThO_2, UO_2, and PuO_2. The lattice constants for these cubic materials were taken from Donnay & Nowacki (1954) and are, $a_0 = 5{\cdot}584$, $a_0 = 5{\cdot}470$, $a_0 = 5{\cdot}397$ Å, respectively, for ThO_2, UO_2, and PuO_2. The theoretical densities were calculated as 10·07, 10·96, and 11·58 g.cm.$^{-3}$ for ThO_2, UO_2, and PuO_2. The mass absorption coefficient for oxygen was taken from the work of Grodstein (1957). The mass absorption coefficients for Th, U, and Pu were taken from previous work by the author (Roof, 1959*b*).

Experimental constants for use in equation (1) are, $l = 1$ cm., $r = 14{\cdot}605$ cm., $\lambda = 0{\cdot}7107$ Å for Mo $K\alpha$, 1·5418 Å for Cu $K\alpha$, 1·9373 Å for Fe $K\alpha$, and 2·2909 Å for Cr $K\alpha$. $N^2 = (1/a_0^3)^2$ and $\omega = 3{\cdot}33 \times 10^{-3}$ sec^{-1}. The theoretical linear absorption coefficients for the respective materials and X-ray wavelengths are given in Table 1.

Table 1. *Theoretical linear absorption coefficients for* ThO_2, UO_2, *and* PuO_2

	Mo $K\alpha$	Cu $K\alpha$	Fe $K\alpha$	Cr $K\alpha$
ThO_2	986·9 cm.$^{-1}$	3731	6288	8622
UO_2	1249·4	4012	6765	8673
PuO_2	557·8	5043	9518	12854

Σ and I_0 for each reflection were determined as outlined in the preceeding section. Experimental data for Σ and I_0, coupled with the experimental constants given above, when inserted in equation (1), yield values for the observed structure factor squared, $|F_0|^2$. The values of the observed structure factor squared are corrected for the effect of temperature by use of equation (2) where the characteristic temperature of ThO_2, UO_2, and PuO_2 is taken as 415 °K. The value of 415 °K. for the characteristic temperature was experimentally determined by the author for PuO_2 (Roof, 1960*b*). This value is assumed to be valid for ThO_2 and UO_2 also on the basis that since all three materials have the same structure (CaF_2) and the average mass of a lattice point is very nearly the same for all three materials then it is not likely that their characteristic temperatures would be significantly different.

Experimental results

Values for the observed structure factor, corrected for the effects of temperature, $|F_T|$, are given in Tables 2, 3, and 4 for ThO_2, UO_2, and PuO_2 for Mo $K\alpha$, Cu $K\alpha$, Fe $K\alpha$, and Cr $K\alpha$ radiation. As an example of the derivation of an atomic scattering factor and of the anomalous dispersion corrections from the data, $|F_T|$, we will consider the derivation of the scattering factor for Pu for Mo $K\alpha$ radiation. For the PuO_2 structure the structure factor, $|F|$, is

Table 2. *The observed structure factor, corrected for temperature,* $|F_T|$, *for* ThO_2 *for* Mo $K\alpha$, Cu $K\alpha$, Fe $K\alpha$, *and* Cr $K\alpha$.

hkl	Mo $K\alpha$	Cu $K\alpha$	Fe $K\alpha$	Cr $K\alpha$
111	314±3	330±6	326±5	293±4
200	248±3	265±3	260±4	226±4
220	312±4	330±3	329±6	297±4
311	251±3	267±4	267±5	237±4
222	211±2	227±4	229±4	195±3
400	256±5	271±5	271±5	243±11
331	215±3	231±4	235±4	204±3
420	187±3	201±2	204±3	177±3
422	220±3	238±3	240±4	—
440	193±3	213±3	212±3	—
531	169±3	187±2	—	—
620	176±2	194±3	—	—
533	156±3	172±2	—	—
622	138±4	155±3	—	—
444	160±5	177±4	—	—

Table 3. *The observed structure factor, corrected for temperature,* $|F_T|$, *for* UO_2 *for* Mo $K\alpha$, Cu $K\alpha$, Fe $K\alpha$, and Cr $K\alpha$.

hkl	Mo $K\alpha$	Cu $K\alpha$	Fe $K\alpha$	Cr $K\alpha$
111	285±3	345±4	317±5	278±6
200	218±3	277±3	248±4	214±3
220	282±3	343±4	315±3	291±7
311	224±3	280±3	254±4	233±4
222	180±4	236±3	213±3	193±5
400	224±5	282±5	264±4	246±6
331	186±3	239±4	220±3	204±7
420	156±3	211±4	190±3	179±3
422	190±2	243±4	225±4	—
440	168±3	220±3	—	—
531	147±3	196±4	—	—
620	148±4	199±3	—	—
533	129±3	179±3	—	—
622	108±4	163±3	—	—
444	134±7	186±4	—	—

Table 4. *The observed structure factor, corrected for temperature,* $|F_T|$, *for* PuO_2 *for* Mo $K\alpha$, Cu $K\alpha$, Fe $K\alpha$, *and* Cr $K\alpha$.

hkl	Mo $K\alpha$	Cu $K\alpha$	Fe $K\alpha$	Cr $K\alpha$
111	302 ± 2	345 ± 5	318 ± 5	292 ± 4
200	242 ± 3	278 ± 4	252 ± 6	230 ± 2
220	298 ± 4	341 ± 3	319 ± 7	303 ± 6
311	236 ± 2	278 ± 4	262 ± 6	248 ± 5
222	200 ± 5	240 ± 6	222 ± 9	210 ± 4
400	243 ± 4	280 ± 5	270 ± 6	260 ± 5
331	197 ± 2	239 ± 3	232 ± 3	220 ± 3
420	174 ± 3	213 ± 3	204 ± 3	193 ± 2
422	200 ± 3	237 ± 5	234 ± 4	—
440	177 ± 5	219 ± 4	—	—
531	149 ± 2	194 ± 3	—	—
620	157 ± 3	199 ± 2	—	—
533	138 ± 3	179 ± 3	—	—
622	121 ± 2	161 ± 3	—	—

related to the scattering factors of Pu and oxygen according to

$$|F|=4(f_{Pu}+2f_O) \quad \text{for } h+k+l=4n \tag{6}$$

$$|F|=4(f_{Pu}) \quad \text{for } h+k+l=2n+1 \tag{7}$$

$$|F|=4(f_{Pu}-2f_O) \quad \text{for } h+k+l=4n+2 \tag{8}$$

Dividing $|F_T|$ by 4 and multiplying the results by the instrument calibration constant k of equation (5) (and Fig. 1,) yields a scattering factor, f, which is correct relative to the scale and shape of the aluminum scattering curve. The curves for $(f_{Pu}+2f_O)$, (f_{Pu}), and $(f_{Pu}-2f_O)$ are shown in Fig. 2.

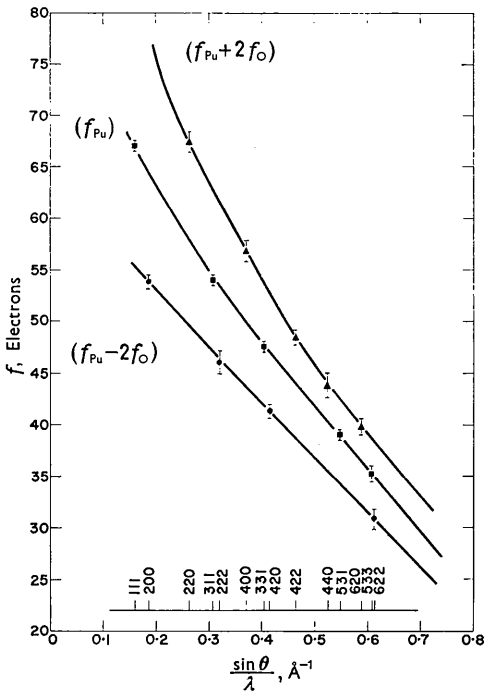

Fig. 2. Scattering curves for $(f_{Pu}+2f_O)$, (f_{Pu}), and $(f_{Pu}-2f_O)$ derived from experimental values of the structure factor, corrected for temperature, $|F_T|$. Mo $K\alpha$ radiation.

In addition to the instrument calibration constant k, the curves for $(f_{Pu}+2f_O)$ and $(f_{Pu}-2f_O)$ contain an internal calibration also, since one-fourth of the dif-

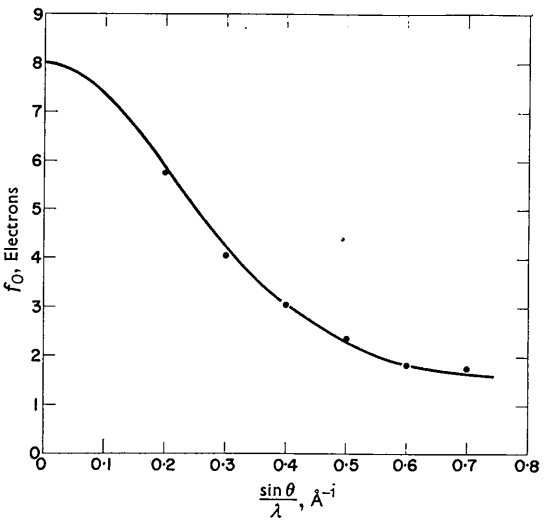

Fig. 3. Comparison between the McWeeney (1951) oxygen scattering curve (——) and the oxygen scattering curve derived (●) as one-fourth the difference between $(f_{Pu}+2f_O)$ and $(f_{Pu}-2f_O)$.

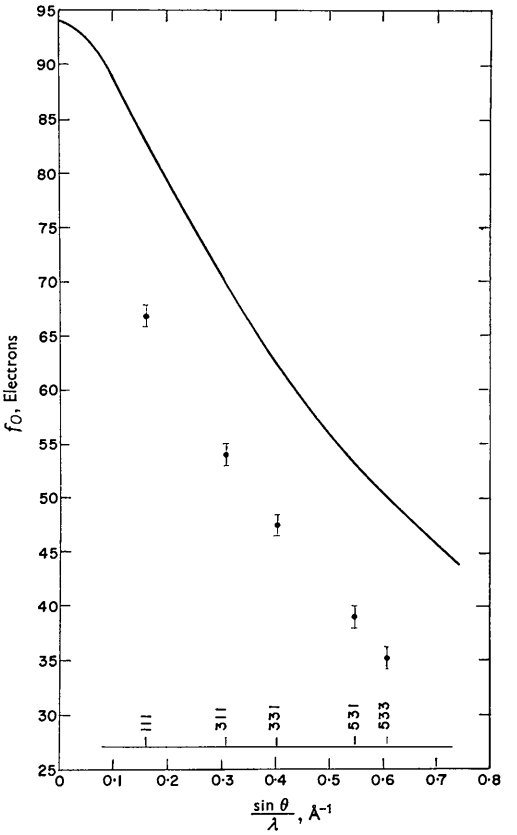

Fig. 4. Comparison between the experimental scattering curve (•) and the TFD scattering curve for Pu. Mo $K\alpha$ radiation.

ference between these two curves yields values for the scattering curve of oxygen. Any absorption edges for oxygen are sufficiently removed from the X-ray wavelengths used that the anomalous dispersion effect for oxygen can be assumed to be negligible. Fig. 3 shows the good agreement between the derived oxygen curve and the oxygen scattering curve according to McWeeney (1951).

In Fig. 4 the scattering curve for Pu, (f_{Pu}), is compared with the TFD scattering curve for Pu. As mentioned in the *Introduction* the difference between the experimental curve and the TFD curve is taken as a measure of the anomalous dispersion correction.

Equation (4) can be written as

$$f=\{(f_M+\Delta f')^2+(\Delta f'')^2\}^{\frac{1}{2}}\,, \qquad (9)$$

where f_M is the true atomic scattering factor for the metal atom. Equation (9) was programmed for an IBM 704 computer so that, for experimental values of f and the associated values of TFD f_M's, a least squares analysis could be performed to obtain values of $\Delta f'$ and $\Delta f''$. For Pu for Mo $K\alpha$ radiation $\Delta f'=-16{\cdot}7\pm0{\cdot}6$ and $\Delta f''=11{\cdot}7\pm2{\cdot}1$. The value of $-16{\cdot}7$ for $\Delta f'$ is in reasonable agreement with values ranging from -17 to -23 suggested by Cromer & Olson (1959) based on the structure analysis of $PuNi_3$.

The procedure described above is applicable only to the metal atom curve. To extract information concerning $\Delta f'$ and $\Delta f''$ from the $M\pm2O$ curves requires a slight modification in the treatment of the data.

Fig. 5 shows the vector diagram for one formula unit, MO_2, relating f_M, the scattering factor for the metal atom, $\Delta f'$ and $\Delta f''$, the real and imaginary parts of the anomalous dispersion corrections to the metal atom, and f_O the scattering factors for the oxygen atoms. Starting with f_M, $\Delta f'$ is added, then $\Delta f''$ is added, then $\pm2f_O$ is added to yield f, the scattering factor for curves (f_M+2f_O) or (f_M-2f_O). See Fig. 2. It can be seen that if the oxygen atoms are eliminated from Fig. 5 (that is, if attention is concentrated on the metal atom curve alone) then the diagram is a vector representation of equation (9).

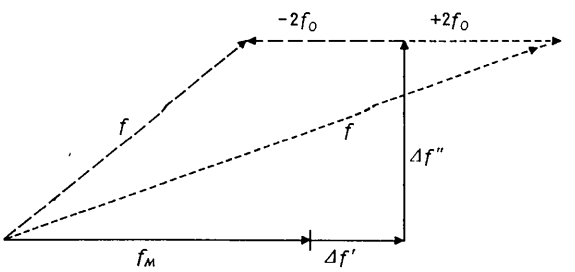

Fig. 5. The vector diagram, for one formula unit, MO_2, relating f_M, the scattering factor for the metal atom, $\Delta f'$ and $\Delta f''$, the real and imaginary parts of the anomalous dispersion correction to the metal atom, and $\pm2f_O$, the scattering factors for the oxygen atoms. f is the resultant scattering factor for either (f_M+2f_O) or (f_M-2f_O). See Fig. 2.

Values for $\Delta f'$ and $\Delta f''$ may be obtained from Fig. 5 in the following manner. Let

$$\sin\alpha=\Delta f''/f \qquad (10)$$

and

$$\cos\alpha=(f_M+\Delta f'\pm2f_O)/f\,. \qquad (11)$$

Since $\sin^2\alpha+\cos^2\alpha=1$, then upon combination of equation (10) and (11) and rearrangement

$$f=\{(f_M+\Delta f'\pm2f_O)^2+(\Delta f'')^2\}^{\frac{1}{2}}\,. \qquad (12)$$

Equation (12) is applicable to all three curves (f_M+2f_O), (f_M), and (f_M-2f_O). It should be noted that for curve (f_M), $f_O=0$, and equation (12) reduces to equation (9). Utilization of equation (12) for the treatment of the experimental data is preferred over equation (9) as equation (12) treats all the data whereas equation (9) is applicable to only about 30% of the total data available. However, once values for $\Delta f'$ and $\Delta f''$ are known, use of equation (9) is very convenient for the calculation of an experimental scattering curve.

Equation (12) was programmed for an IBM 704 computer so that, for experimental values of f, and the associated values of TFD f_M's and the McWeeney oxygen scattering curve, a least squares analysis could be performed to obtain values for $\Delta f'$ and $\Delta f''$.

In Table 5 are given the TFD f_M's for Th, U, and Pu, taken from the work of Thomas, Umeda & King (1958). Values of $\Delta f'$ and $\Delta f''$ derived for Th, U, and Pu for Mo $K\alpha$, Cu $K\alpha$, Fe $K\alpha$, and Cr $K\alpha$ are given in Table 6. Inserting in equation (9) the appropriate quantities given in Tables 5 and 6 allows the experimental scattering curve to be readily calculated.

Table 5. *Thomas–Fermi–Dirac scattering curves for* Th, U, *and* Pu.

$\sin\theta/\lambda$	Th	U	Pu
0	90	92	94
0·05	88·60	90·58	92·56
0·10	84·97	86·90	88·83
0·15	80·32	82·18	84·05
0·20	75·67	77·42	79·22
0·25	71·21	72·93	74·66
0·30	67·06	68·71	70·37
0·35	63·16	64·74	66·33
0·40	59·57	61·09	62·60
0·50	53·27	54·66	56·05
0·60	47·90	49·17	50·45
0·70	43·34	44·51	45·69
0·80	39·42	40·50	41·59

Discussion

In Fig. 6, data from Table 6 is plotted as a function of $\lambda/\lambda_{L_{III}}$, where λ is the incident radiation and $\lambda_{L_{III}}$ is the wavelength of the L_{III} absorption edge. In Fig. 7, data from Table 6 is plotted as a function of $\lambda/\lambda_{M_IM_{II}}$ where λ is the incident radiation and $\lambda_{M_IM_{II}}$ is the average of the wavelengths of the M_I and M_{II} absorption edges. Since the difference between

the M_I and M_{II} absorption edges for Th, U, and Pu amounts to approximately 5 per cent of the value of either the M_I or the M_{II} absorption edge, an average is justifiable for a graphic representation. The absorption edges were taken from the work of Richtmyer & Kennard (1947). The L_{III} absorption edge is 0·76, 0·72 and 0·68 Å for Th, U, and Pu respectively. The M_I, M_{II} averages are 2·52, 2·28 and 2·14 Å for Th, U, and Pu respectively.

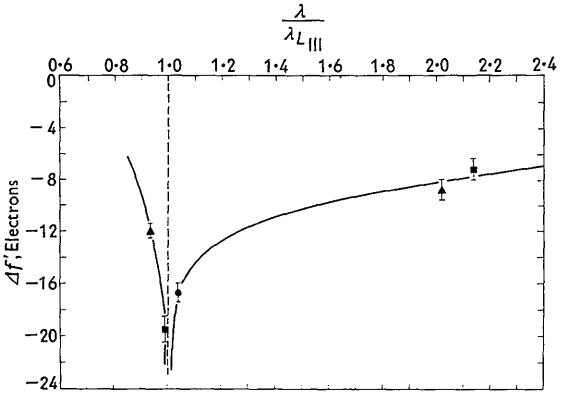

Fig. 6. The variation of $\Delta f'$ as a function of $\lambda/\lambda_{L_{III}}$. Thorium (▲), Uranium (■), Plutonium (●).

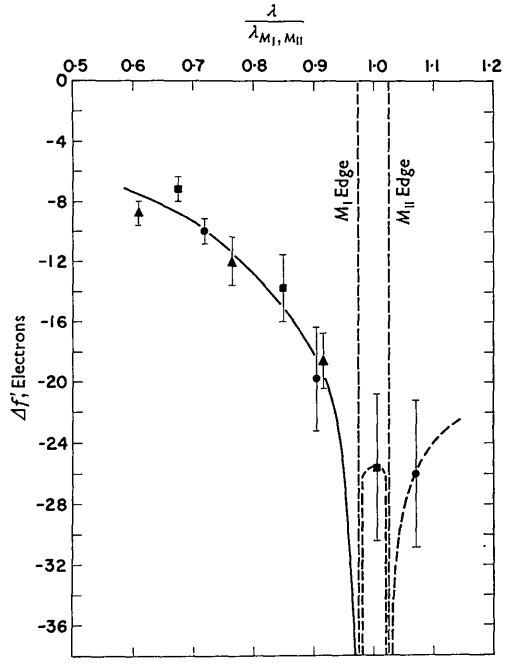

Fig. 7. The variation of $\Delta f'$ as a function of $\lambda/\lambda_{M_I, M_{II}}$. Thorium (▲), Uranium (■), Plutonium (●).

Figs. 6 and 7 indicate general trends for the behavior of anomalous dispersion in the region of wavelengths and elements covered, although the number of experimental points might be considered less than adequate for definite conclusions. In general, a marked decrease in the value of the scattering factor, f, is found for wavelengths in the immediate neighborhood of an absorption edge of the scatterer under consideration. This is illustrated in Fig. 6 for Th, U, and Pu for Mo $K\alpha$ radiation, with the result that the closer the degree of approach to $\lambda/\lambda_{L_{III}}=1{\cdot}0$, the greater the decrease in the scattering factor. For values of $\lambda/\lambda_{L_{III}}$ much greater than 1·0 the trend is for $\Delta f'$ to approach the oscillator strength of the L electrons, g_L, for which Hönl (James, 1948) has computed a value of 4·5 electrons.

In Table 7 are listed values of $\Delta f'$ and $\Delta f''$ for Th, U, and Pu based on calculations made by Dauben & Templeton (1955). As Dauben & Templeton point out, these values are based on equations, the constants of which were determined utilizing tungsten, $Z=74$. Extrapolation of these equations to the region of $Z=90$ to 94 may not be justified.

Table 6. *Experimental values of $\Delta f'$ and $\Delta f''$ for* Th, U, *and* Pu

Based on the TFD scattering curves for Th, U, and Pu utilized as theoretical standards

		Mo $K\alpha$	Cu $K\alpha$	Fe $K\alpha$	Cr $K\alpha$
Th	$\Delta f'=$	$-12{\cdot}0\pm0{\cdot}4$	$-9{\cdot}3\pm0{\cdot}6$	$-12{\cdot}0\pm1{\cdot}7$	$-18{\cdot}6\pm1{\cdot}7$
	$\Delta f''=$	$14{\cdot}4\pm1{\cdot}2$	$18{\cdot}9\pm1{\cdot}6$	$25{\cdot}5\pm3{\cdot}4$	$22{\cdot}3\pm3{\cdot}6$
U	$\Delta f'=$	$-19{\cdot}5\pm0{\cdot}8$	$-6{\cdot}8\pm0{\cdot}8$	$-13{\cdot}8\pm2{\cdot}1$	$-25{\cdot}6\pm4{\cdot}7$
	$\Delta f''=$	$12{\cdot}9\pm2{\cdot}5$	$16{\cdot}0\pm2{\cdot}5$	$20{\cdot}0\pm5{\cdot}4$	$30{\cdot}5\pm6{\cdot}3$
Pu	$\Delta f'=$	$-16{\cdot}5\pm0{\cdot}6$	$-9{\cdot}5\pm0{\cdot}8$	$-19{\cdot}8\pm3{\cdot}4$	$-26{\cdot}0\pm4{\cdot}8$
	$\Delta f''=$	$10{\cdot}0\pm2{\cdot}7$	$20{\cdot}3\pm1{\cdot}9$	$32{\cdot}6\pm5{\cdot}0$	$34{\cdot}7\pm5{\cdot}9$

Table 7. *Theoretical values of $\Delta f'$ and $\Delta f''$ for* Th. U, and Pu

Based on the calculations of Dauben & Templeton (1955)

		Mo $K\alpha$	Cu $K\alpha$	Fe $K\alpha$	Cr $K\alpha$
Th	$\Delta f'=$	−7	−5	*	−15
	$\Delta f''=$	8	13	*	25
U	$\Delta f'=$	−8	−5	*	−19
	$\Delta f''=$	8	15	*	28
Pu	$\Delta f'=$	*	−5	*	*
	$\Delta f''=$	5	16	*	*

* Not calculated.

Comparison of identical items in Table 7 with those in Table 6 reveals, however, that the experimental terms all have the correct signs indicated by theory and that the experimental numbers are of the same order of magnitude as those indicated by theory. Thus, the agreement between experiment and theory can best be described as qualitative.

Townsend, Jeffrey & Pangis (1959) presented a formula by which $\Delta f''$ may be calculated for any element if the mass absorption coefficient of the element is known. This formula may be written as

$$\Delta f''=(1/2\lambda r_0).(A/N).\mu_m \qquad (13)$$

where

λ = X-ray wave length, cm.,
$r_0 = e^2/mc^2 = 2{\cdot}81784 \times 10^{-13}$ cm.,
A = atomic weight,
N = Avogadro's number, $6{\cdot}02472 \times 10^{23}$ mol.$^{-1}$,
μ_m = mass obsorption coefficient, cm.^{2}g.$^{-1}$.

Table 8. *Comparison between observed and calculated values for $\Delta f''$*

Calculated values according to the formula of Townsend, Jeffrey & Pangis (1959)

		Mo $K\alpha$	Cu $K\alpha$	Fe $K\alpha$	Cr $K\alpha$
Th	$\Delta f_o''$	$14{\cdot}4 \pm 1{\cdot}2$	$18{\cdot}9 \pm 1{\cdot}6$	$25{\cdot}5 \pm 3{\cdot}4$	$22{\cdot}3 \pm 3{\cdot}6$
	$\Delta f_c''$	10·6	18·4	24·6	28·6
U	$\Delta f_o''$	$12{\cdot}9 \pm 2{\cdot}5$	$16{\cdot}0 \pm 2{\cdot}5$	$20{\cdot}0 \pm 5{\cdot}4$	$30{\cdot}5 \pm 6{\cdot}3$
	$\Delta f_c''$	12·6	18·6	25·0	27·1
Pu	$\Delta f_o''$	$10{\cdot}0 \pm 2{\cdot}7$	$20{\cdot}3 \pm 1{\cdot}9$	$32{\cdot}6 \pm 5{\cdot}0$	$34{\cdot}7 \pm 5{\cdot}9$
	$\Delta f_c''$	5·4	22·5	33·9	38·7

As an example we will consider the calculation of $\Delta f''$ for Pu for Cu $K\alpha$ radiation. $\lambda = 1{\cdot}5418 \times 10^{-8}$ cm., $A = 242$, and $\mu_m = 488$ cm.^{2}g.$^{-1}$ and the calculated $\Delta f'' = 22{\cdot}5$, which is in good agreement with the observed value of $\Delta f'' = 21{\cdot}0 \pm 1{\cdot}9$. Table 8 lists these values along with the calculated and observed $\Delta f''$ for the other elements and radiations. Considering the difficulty in obtaining observed values of $\Delta f''$ and the assumptions involved in the theoretical formula, (equation (13) being strictly valid only for $\sin\theta/\lambda = 0$), the agreement is quite good and in this case may be described as semi-quantitative.

The author wishes to acknowledge the assistance of R. H. Moore of this Laboratory for his statistical application of least squares fitting to nonlinear functions, and the helpful comments and criticisms of Prof. K. N. Trueblood and Prof. D. H. Templeton.

References

CHIPMAN, D. & PASKIN, A. (1960). *J. Appl. Phys.* **31**, 1130.

CROMER, D. T. & OLSEN, C. E. (1959). *Acta Cryst.* **12**, 689.

DAUBEN, C. H. & TEMPLETON, D. H. (1955). *Acta Cryst.* **8**, 841.

DONNAY, J. D. H. & NOWACKI, W. (1954). *Crystal Data*, Geological Society of America, New York.

GRODSTEIN, G. W. (1957). Attentuation Coefficients from 10 kev to 100 Mev, National Bureau of Standards, Circular No. 583, U.S. Government Printing Office, Washington, D.C.

JAMES, R. W. (1948). *The Optical Principles of the Diffraction of X-rays*, p. 160. London: Bell.

MCWEENEY, R. (1951). *Acta Cryst.* **4**, 513.

PARRY, G. S. (1955). *Acta Cryst.* **4**, 593.

RICHTMYER, F. K. & KENNARD, E. H. (1947). *Introduction to Modern Physics*, p. 485, 4. ed. New York: McGraw-Hill.

ROOF, R. B., Jr. (1959*a*). *J. Appl. Phys.* **30**, 1599.

ROOF, R. B., Jr. (1959*b*). *Phys. Rev.* **113**, 820.

ROOF, R. B., Jr. (1960*a*). *J. Appl. Phys.* **31**, 1131.

ROOF, R. B., Jr. (1960*b*). *J. Nuclear Materials*, **2**, 39.

TOWNSEND, J. R., JEFFREY, G. A. & PANGIS, G. N. (1959). *Z. Kristallogr.* **112**, 150.

THOMAS, L. H., UMEDA, K. & KING, K. (1958). (Unpublished work.)

Acta Cryst. (1961). **14**, 940

The Refinement of the Structure of the Complex of Iodine with 1,4-Diselenane, $C_4H_8Se_2 . 2\,I_2$

BY GEORGE Y. CHAO* AND J. D. MCCULLOUGH

Department of Chemistry, University of California at Los Angeles, Los Angeles 24, California, U.S.A.

(*Received* 16 *November* 1960)

The structure of the molecular complex $C_4H_8Se_2 . 2\,I_2$ has been refined by three-dimensional, full-matrix least-squares procedures. There are two molecules of the complex in the unit cell which has the dimensions:

$$a = 6{\cdot}876 \pm 0{\cdot}007,\ b = 6{\cdot}325 \pm 0{\cdot}007,\ c = 17{\cdot}68 \pm 0{\cdot}01\ \text{Å};\ \beta = 118°30' \pm 20'.$$

The space group is $P2_1/c$. The molecules are thus required only to be centrosymmetric but the molecular symmetry is actually $2/m$ within the standard deviations. The observed bond distances and angles are: I_1–$I_2 = 2{\cdot}870 \pm 0{\cdot}003$, I_2–Se $= 2{\cdot}829 \pm 0{\cdot}004$, Se–$C_1 = 1{\cdot}947 \pm 0{\cdot}024$, Se–$C_2 = 1{\cdot}980 \pm 0{\cdot}024$, C_1–$C_2 = 1{\cdot}568 \pm 0{\cdot}030$ Å; I_1–I_2–Se $= 180{\cdot}0 \pm 0{\cdot}3°$, I_2–Se–$C_1 = 101{\cdot}5 \pm 1{\cdot}0°$, I_2–Se–$C_2 = 100{\cdot}5 \pm 1{\cdot}0°$, C_1–Se–$C_2 = 100{\cdot}5 \pm 1{\cdot}8°$, Se–$C_1$–$C_2' = 117{\cdot}2 \pm 2{\cdot}0°$, Se–$C_2$–$C_1' = 113{\cdot}0 \pm 2{\cdot}0$.

The structure of the diselenane part of the molecule is but slightly changed by complexing with iodine, however, the I–I bond in the complex is 0·21 Å longer than that in solid I_2. In contrast to the equatorial bonding of iodine to sulfur in the dithiane complex, the iodine is bonded to selenium in axial positions in the diselenane complex.

Introduction

A preliminary study of the structures of the iodine complexes of 1,4-dithiane and 1,4-diselenane (McCullough, Chao & Zuccaro, 1959) and the three-dimen-

* Present address: Department of Geology, Carleton University, Ottawa, Canada.